RESEARCH PAPER

Panel Shear of Plywood in Structural Sizes - Assessment Improvement Using Digital Image Correlation

J. Viguier[1] · B. Marcon[1] · J. C. Butaud[1] · L. Denaud[1] · R. Collet[1]

Abstract

This paper introduces a new test configuration for the determination of panel shear properties in structural sizes. This original test configuration has been successfully applied to calculate the shear properties of beech plywood. A numerical model has been developed to evaluate the influence of such a novel setup in comparison to the common standard. The research includes the mechanical characterization of a total of 36 samples using Digital Image Correlation (DIC) to measure the in plane displacements. The use of DIC has been proven to be efficient to measure the shear properties and also acts as a tool to ensure that the solicitation was adequate during the test. Finally, the results highlight the interest to actually perform the proposed test instead of using the alternative density-based equivalencies provided by the standards.

Keywords Shear · DIC · Beech · Plywood

Introduction

Plywood is often used in the construction sector. In particular, high quality beech plywood could exibit great features to be used in the construction for plywood gussets in nailed or glued trusses or as a web of I-Joist. Therefore obtaining reliable shear properties for plywood is essential to ensure security and cost efficiency in the legal range of the building standards. The measured shear properties has not been found to be a constant value [1], but appears to be affected by the method of shear properties determination even when controlling all factors which normally affect the mechanical properties of wood. The evaluation of shear properties has conducted to create a wide range of standardized and non-standardized test methods (two rails, plate shear, bending tests, torsion, ...). Among those, the two rails type seems to be preferred in order to test plywood in structural size. During this test, the load is transferred to the specimen through two pair of rails glued or bolted parallel to its longer edge in such a way that the shear is nearly pure in the central area. Several studies [2–6] have been conducted over the years to develop or assessing the difference between two-rails type tests.

The area exposed to shear has been kept nearly constant over the years to a rectangle of approximately 200 by 600 mm^2. Different strategies to perform this test have been experienced, all of them requiring complicated apparatus (see Fig. 1). In the latest European standard (EN 789 [7]), this area has been changed to a more complicated shape with a slightly lower area (see Fig. 1(c)) but the principle and the complexity remain constant. This complexity probably causes the lack of values issued from plywood performance declaration of the majority of the plywood panel manufacturers. Indeed, the producers prefer to use density equivalencies given in EN 12369-2 [8] to provide shear properties even if they are very penalizing and do not reflect the true mechanical properties of plywood panels especially in the case of beech.

Panels shear modulus is usually measured using a Linear Variable Differential Transformer (LVDT) orientated by 45° across the central area (symbolized by a rectangle in Fig. 1) on each side of the specimen and then averaged. Timbers shear modulus can also be determined through flexural [9] or torsional [10] vibration mechanical tests with accelerometers and more or less complex finite elements analysis (FEA). In this study, Digital Image Correlation (DIC) is proposed as an alternative to the fixation of LVDT and as a substantial improvement to measure those displacements. In the past 30 years, DIC has proved to be

Q1

✉ J. Viguier
joffrey.viguier@gmail.com

Q2

[1] LaBoMaP, Arts et Metiers Institute of Technology, LaBoMaP, HESAM Université, rue Porte de Paris, F-71250, Cluny, France
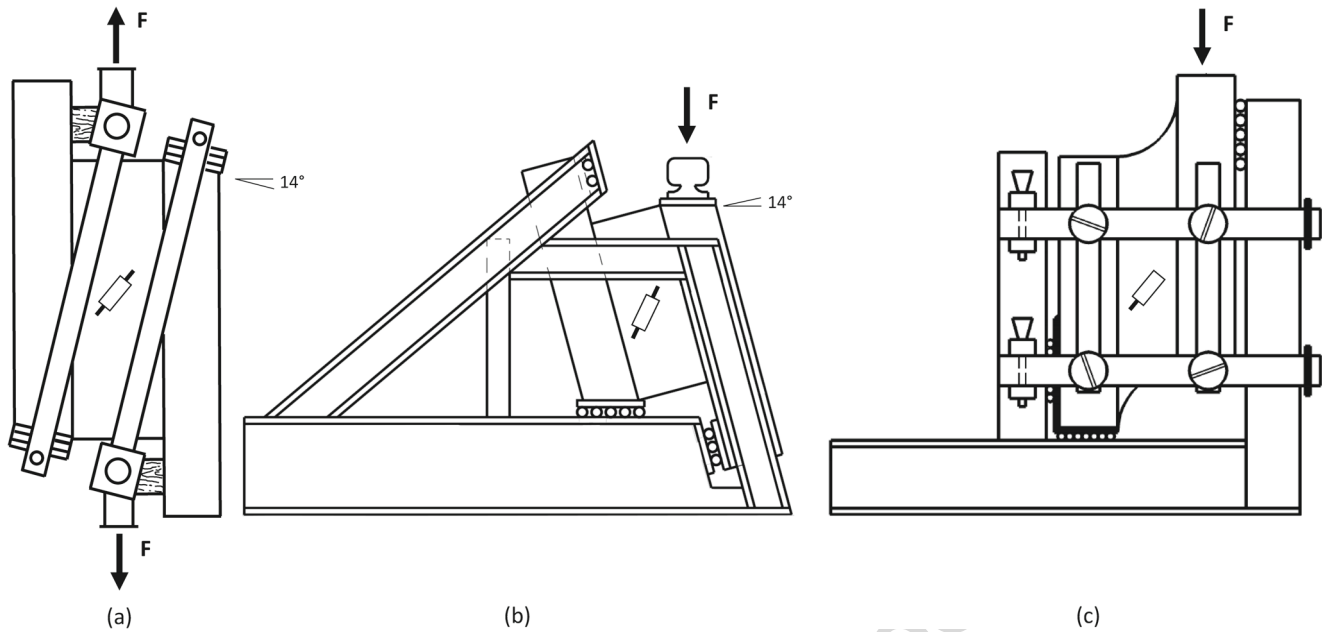
Fig. 1 Different two-rails configuration tests used or in use within the past 30 years

a very valuable non-invasive tool for full-field displacement measurements [11–14] and its accuracy has been proven [15]. The use of DIC in the field of wood testing is increasing [16–18].

The main objective of the present study is to propose a simpler method to determine the shear properties of wooden panels and more particularly plywood ones. In addition an experimental part designed to validate the modified test using full field measurements, finite elements numerical simulations have been used to determine the influence of using the proposed test method on the mechanical properties of the plywood panels.

Materials and Methods

Sampling

A total of 18 beech plywood panels were used for this study and two different thicknesses (18 and 25 mm with respectively 9 and 11 plies) have been studied. Samples were cut using a three-axis router machine according to the shape described in Fig. 2. In order to define a test which can be performed easier than the one described in the standard [7], involving a less bulky setup, the chosen strategy was to tilt the sample. For the experimental part, the angle α has been taken equal to 18°   in such a way that the moment is nearly equal to 0. In doing so, the special apparatus described in the standard was not needed anymore and the initially complex test looks like a simple self balanced compression test. Four Douglas-fir timber

rails with a thickness equals to 35 mm have then been glued using polyvinyl acetate (PVAC) to each specimen to avoid buckling of the sample during the test as required by the standard [7]. Two samples have been cut from each panel : one having its external ply with fiber along the longest dimension and the second one perpendicular to its longest dimension. Finally, 36 samples have been made.

Mechanical Test and Displacements Measurement

The tests were performed with a Zwick Roell static material testing machine with a 250 kN load cell. The load was applied on the top surface of the timber rails with an adjusted application rate, so that the maximum load was reached within 300 $\pm$ 120 s according to EN 789 [7]. In practice, the loading rate has been chosen equals to 2 mm/min. The shear deformation was measured on both faces in the middle of the specimen using 2D digital image correlation. Images of both faces and their corresponding load were recorded during the whole test. Digital frames of both sides of the specimen were recorded using two Basler ace acA1920-155um type imagers equipped with Pentax Ricoh FL-CC3516-2M - 1.6 / 35 mm lenses. Those cameras exhibit a resolution of 1920 by 1200 square pixels with a pitch size of $5.86e^{-3}$ mm^2. The observed area was set to 211 by 132 mm^2 thanks to extension tubes with a working distance (standoff distance) of 1 meter. The scene was illuminated using identical white LED projectors on both sides and a built-in lens diaphragm used to reach identical grey level repartition histograms for both sides of the specimen. The geometrical centres had been marked

Fig. 2 Experimental test setup

Fig. 3 **a** beech natural pattern for DIC on one sample showing medullary rays (elliptical darker shapes), **b** corresponding X-and Y-displacement fields obtained between the first image and the reference image, **c** DIC pseudostatic accuracy assessment from 10 consecutive images taken free from loading
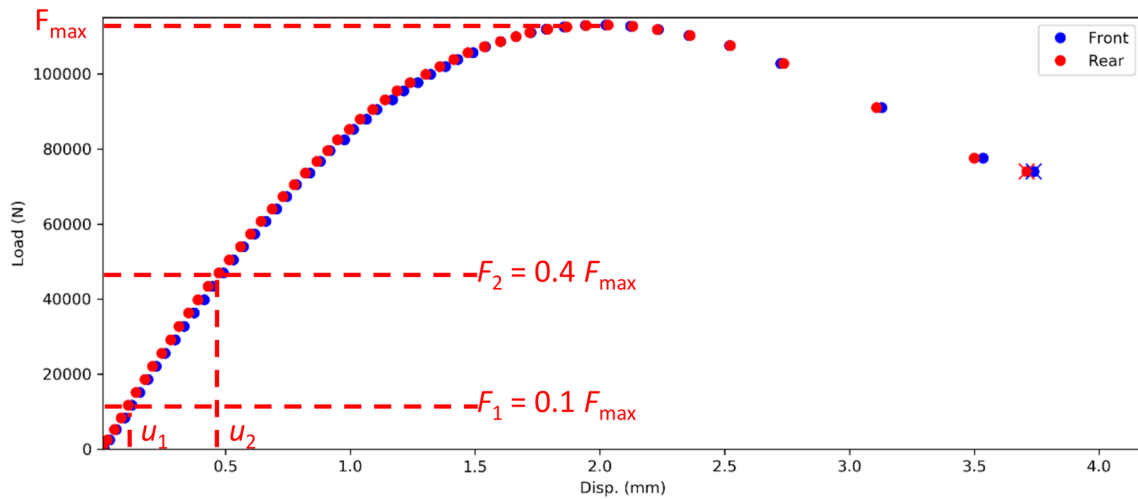
Fig. 4 Typical load-displacement curves (front and rear) used for the panel shear properties assessments. The displacement represents the distance measured by DIC between two points located on the compression diagonal at 45° to the rails passing through the centre of the shear area

precisely on both sides of the specimen and centred on both camera respective fields of view before tests were performed (see Fig. 3(a)). Moreover, the alignment of the camera axis with the specimen ones, as represented in the Fig. 2, was ensured by imposing their correspondence with the anti-buckling beams, and the camera orientation (sensor parallel with the observed area) was checked using a grid calibration plate. The magnification factor obtained with such experimental set up was 9.08 px/mm (or 0.11 mm/px). Hardware and software resources have been developed specifically to record simultaneously the load value and its corresponding pictures. The experimental test setup is described in Fig. 2.

The principle of Digital Image Correlation is to compare digitized images of non-deformed specimen (reference) to multiple images of the same specimen while applying the loading to obtain the full-field displacement. An important element of the measurement procedure is the image analysis software package which is supposed to provide an apparent 2-D displacement field that maps a so-called "reference image" to a "deformed image" at a discrete set of positions, according to the principle of optical flow conservation. The displacement was computed using the image analysis software, DaVIS 10.0.5, by LaVision. In the case of this study, no surface preparation of the observed area has been done, the medullary rays of beech as shown in (Fig. 3(b)) have been directly used as the pattern from which to correlate the images between two successive loading steps. The subsetsize and the stepsize have been taken equal to 51 and 17 pixels respectively. The region of interest is shown in Fig. 2. The image acquisition frequency was fixed at 0.2 Hz.

The natural pattern the beech plywood featured, see (Fig. 3(a)), appeared as really satisfying among the different surface preparation considering the difficulty to master the paint application on big amount of samples compared to the accuracy required for the shear modulus determination (some details regarding this will be discussed in Section "Mechanical Properties Calculation"). Nonetheless, the natural pattern of beech veneer is anisotropic due to the presence of elliptic and oriented medullary rays affecting the correlation error which becomes anisotropic correspondingly.

Table 1 Material properties used in finite elements analysis

Property	Ply material (beech) [20]	Wood support (Douglas fir) [21]
E_X (MPa)	14000	14740
E_Y (MPa)	1160	737
ν_{XY}	0.45	0.45
G_{XY} (MPa)	1080	1150
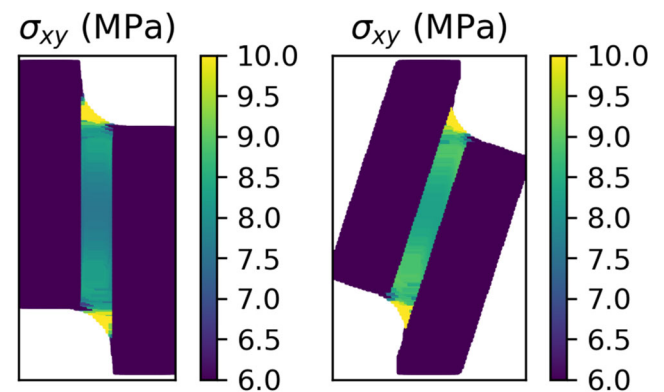
Fig. 5 Comparison of the modeled strain field obtained from vertical and tilted samples
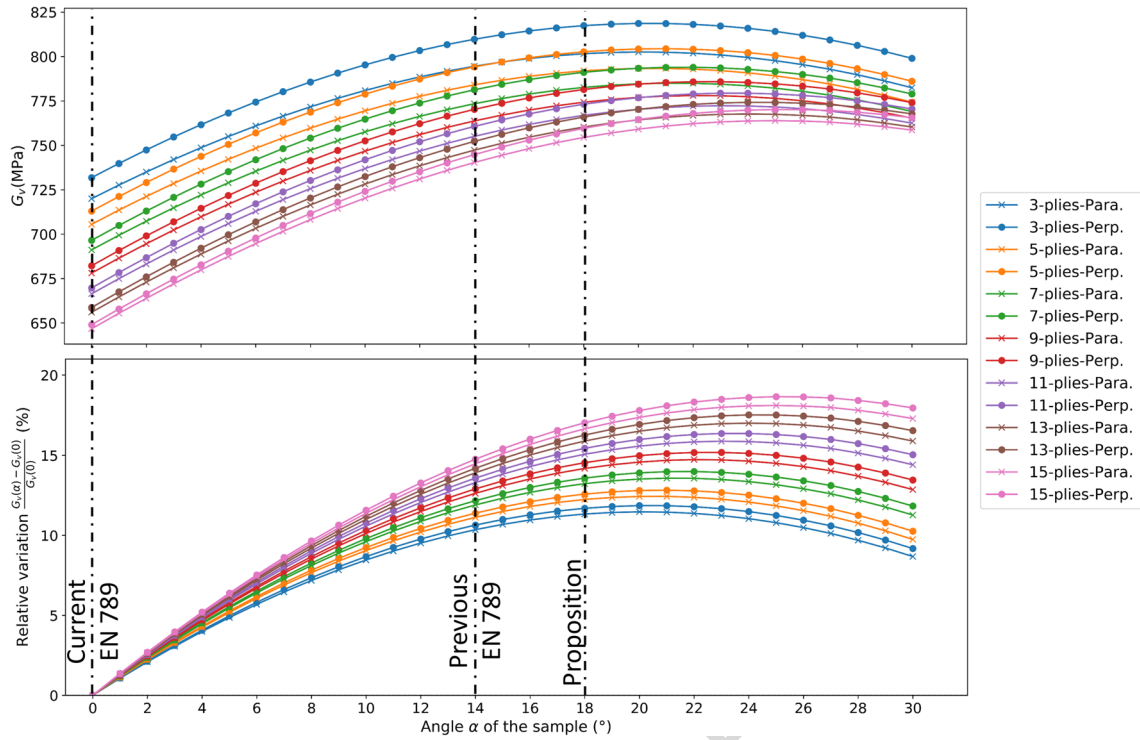
Fig. 6 Influence of tilting the sample at different angle on the calculation of G_v. The results for two types of sample (Parallel and Perpendicular) and different thicknesses are presented. The upper part shows the calculated G_v and the lower part the relative variation observed with the configuration without tilting the sample

146 The average correlation error is determined using the
147 10 images taken before the loading is applied for each
148 sample, performing a DIC computation on them under the
149 exact same calculation settings (subset size 51 pixels and
150 step size 17 pixels), and extracting the standard deviation
151 at 68% confidence interval of the X- and Y-displacement
152 fields obtained for those non-deformed configurations. An
153 example is provided in (Fig. 3(b)). Thus, the average
154 displacement field error, arising from the whole samples
155 batch on both sides, were $\pm$ 4.4E^{-3} mm ($\pm$ 0.02 pixel)
156 and $\pm$ 2.2E^{-3} mm ($\pm$ 0.01 pixel) respectively for the
157 medullary rays direction and its normal one displayed by
158 (Fig. 3(b) and (c)). Those values embed the pattern quality,
159 the enlightenment intensity variations and the eventual
160 whole system vibrations (rigid body displacement between
161 the sample and the cameras). The influence of this error on
162 the calculation of the shear modulus will be discussed later.

Mechanical Properties Calculation

164 The calculation of the shear modulus is based on
165 load-displacement curves. The displacement is measured
166 between two selected positions on the images. Those two
167 positions were located on the compression diagonal at 45°
168 to the rails passing through the centre of the shear area. The
169 distance between the two points is equal to 120 mm and

170 corresponds to the theoretical position of the extensometer
171 prescribed in EN 789 [7] (see Fig. 2).

172 The invasive attachment of a physical extensometer with
173 pins inserted in holes is not necessary thanks to the use of
174 DIC. An example on a load-displacement curves obtained
175 on the two faces of the sample is described in Fig. 4. The
176 section of the graph between $0.1F_{max}$ and $0.4\ F_{max}$ is
177 used for a linear regression analyses and the panel shear
178 modulus of rigidity is then calculated using (equation (1)).
179 This equation is similar to the one given in the standard
180 except for the $cos(\alpha)$ term introduced to take into account
181 the tilting angle [7].

$$G_v = \frac{0.5cos(\alpha)(F_2 - F_1)l_1}{(u_2 - u_1)lt} \tag{1}$$

where: 182

- $(F_2 - F_1)$ is the increment of load between $0.1F_{max}$ and   183
  $0.4F_{max}$ in N,   184
- $(u_2 - u_1)$ is the increment of deflection corresponding   185
  to $(F_2 - F_1)$ using a linear regression in mm,   186
- l_1 is the distance between the two selected points and is   187
  equal to 120 mm,   188
- l is the length of the test piece measured along the centre   189
  line of the shear area (including the radius section) in   190
  mm,   191
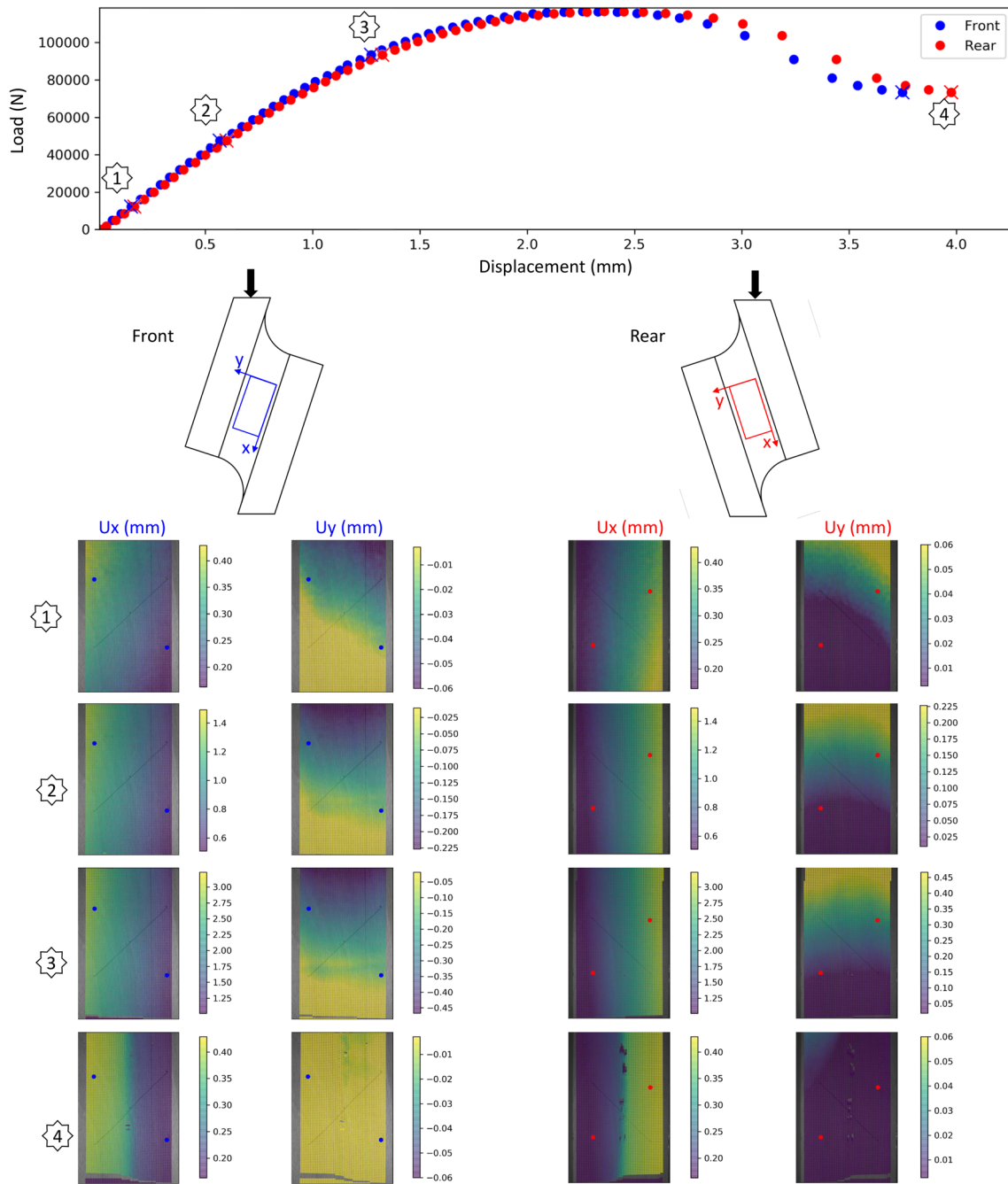
Fig. 7 Typical results of a shear test. The upper part represents the load-displacement curve during the test. Four levels of solicitation are highlighted and their respective displacement fields for both sample sides and two directions are presented in the lower part

192 – t is the average thickness of the test piece measured at
193   two points along the centre line of the shear area in mm,
194 – α is the tilting angle of the sample in °.

195   An analysis of the error sources to determine the shear
196 modulus G_v from (equation (1)) leads to a relative error on

the shear modulus of 1.4 % with the following individual 197
error (experimentally determined or from device calibration 198
certificates): $\Delta\alpha = \pm 1°$; $\Delta F = \pm 0.5\% F = \pm 344$ N; 199
$\Delta u = \pm 4.9E\text{-}3$ mm; $\Delta l1 = \pm 0.5$ mm; $\Delta l = \pm 1$ mm; Δt 200
$= \pm 0.01$ mm. This determined Gv error is mostly affected 201
by the displacement one but remains very low, sustaining 202

Fig. 8 Comparison of displacements fields obtained on the front side experimentally by DIC and numerically by FEM
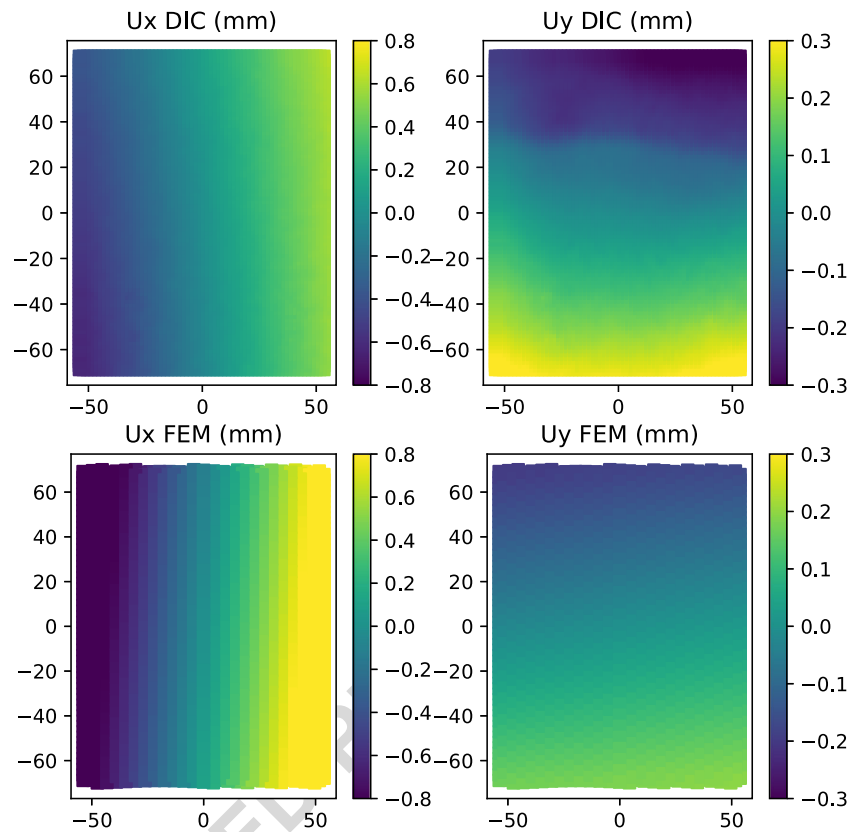
203 the applicability of DIC method using directly the natural
204 beech wood aspect (medullary rays) as pattern (no surface
205 preparation as paint speckle needed).

206   The panel shear strength is calculated from (equation (2))
207 where F_{max} is the maximum load applied up to failure. In this
208 case too the equation only differs by the $\cos(\alpha)$ term [7].

$$f_v = \frac{F_{max}\cos(\alpha)}{lt} \tag{2}$$

209 **Numerical Model**

210 To evaluate the influence of the test modification, a
211 model has been developed using quadratic triangular
212 elements (6-nodes) with orthotropic material properties.
213 The finite element solver used for this study is CAST3M
214 2019 [19], the mechanical software developed by the
215 CEA (French Atomic Energy and Alternative Energies
216 Commission). The grain directions between the different
217 plies were alternatively 0° and 90° to fit with plywood
218 panel composition. The performed simulations were linear
219 regarding the material properties and deflections. The
220 boundary conditions were as follows: for the lower support,
221 displacements were locked in both directions (X and Y),
222 and in the upper support displacements were locked in
223 horizontal direction (X). The tilting angle of the sample
224 varies between 0° and 30°, and the number of plies
225 varies between 3 and 15. The thickness of each ply has been

226 taken equal to 2 mm. The material properties used in the
227 calculations are shown in Table 1 and were taken from the
228 literature [20, 21]. X and Y directions being respectively the
229 fiber direction and the direction perpendicular to the fiber.
230 Given the purpose of the model, the interface between the
231 plies is not modeled.

232   In addition, two types of specimens were modeled in
233 a similar way to the normative recommendations: test
234 specimens with their face grain angle oriented parallel to
235 the load (called type Parallel), and specimens with their face
236 grain angle oriented perpendicular to the load (called type
237 Perpendicular).

Results and Discussions

Results of the Numerical Model

240 The comparison of the shear stress fields, for the same
241 displacement of the loading head, obtained thanks to the
242 FEM after tilting the sample is given in Fig. 5. The different
243 fields were really close to each other either quantitatively
244 or qualitatively. The shear stress in the middle part of the
245 sample is nearly constant in both cases and validate the
246 sample tilting strategy.

247   The shear modulus of rigidity calculated for each
248 simulation is presented in Fig. 6. As one of the model

Fig. 9 Distance between the failure position identified using DIC and the geometric centre of the sample. The upper part is related to 18 mm thick samples and the lower part show the results for 25 mm thick samples
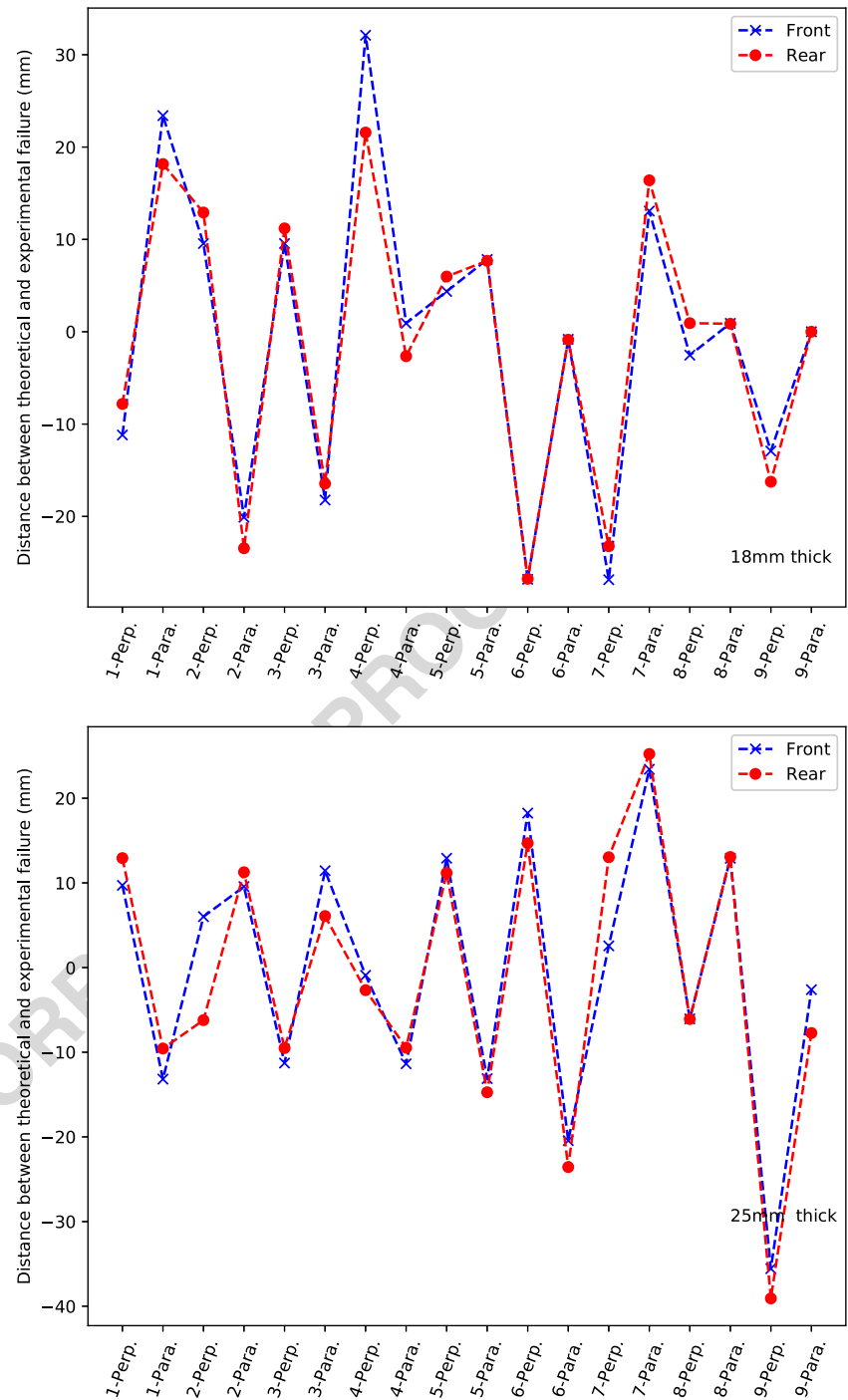
outcomes, it can be seen that the sample type Perpendicular has a higher shear modulus than the Parallel type. The difference observed between the sample types is higher for panels with a lower number of plies. These results highlight the homogenization process that occurs by increasing the number of plies. The shear modulus of rigidity is lower as the number of plies increases. The modeled shear modulus is increasing as the angle of the sample increases until it reaches a maximum value (from 20° to 26° depending on the number of plies), then it decreases as the angle continues to increase. The relative variation of the shear modulus of rigidity for several tilting angles compared to the simulation with the non tilted configuration ($\alpha = 0°$) is presented in Fig. 6. The variation is inferior to 20% in every cases. As the number of plies increases the relative variation also increases. The relative variation for an angle of 18°

Fig. 10 Comparison of the shear modulus calculated on both side of the sample. The upper part is related to 18 mm thick samples and the lower part shows the results for 25 mm thick samples
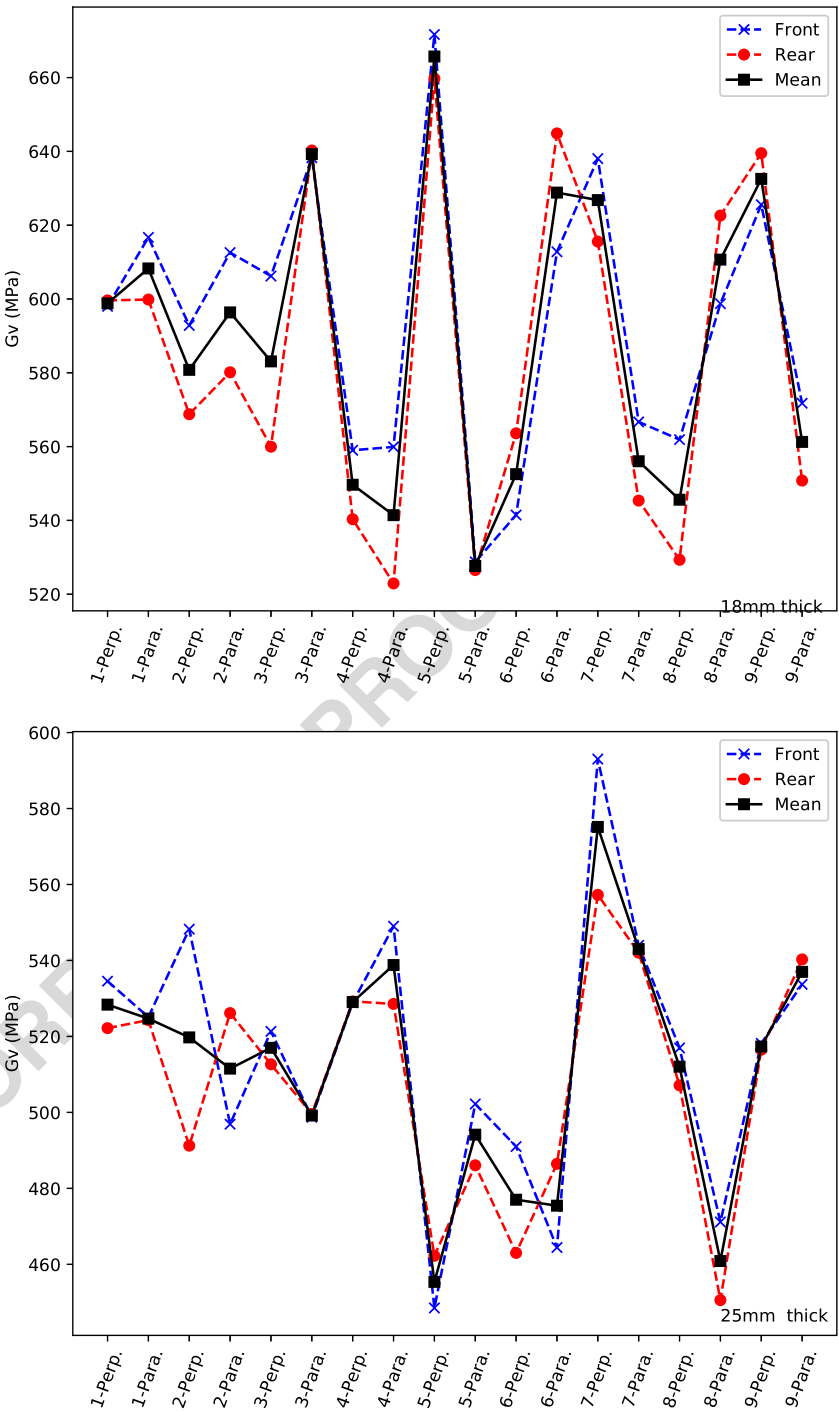
is comprised between 11% and 17% for every modeled cases. This value has to be compared to a relative variation comprised between 10% and 15% for an angle equal to 14° as it was in the previous standard EN 789 (Fig. 1(b)).

Displacement Field and Shear Solicitation

The typical results obtained for a single test are presented in Fig. 7 (18 mm thick and Parallel type panel). The load-

Table 2 Minimum, mean, maximum, 5% percentiles values, standard deviations and coefficient of variation for different characterized properties

	Min	5% quant.	Mean	Max	SD	CV (%)
Density (kg.m^{-3})						
18 mm thick.	661.9	682.4	717.7	752.2	18.3	2.5
Para.	699.7	695.5	720.7	741.2	11.9	1.6
Perp.	661.9	664.8	714.8	752.2	23.4	3.3
25 mm thick.	699.9	699.8	729.8	755.3	15.5	2.1
Para.	702.9	695.9	731.2	755.3	16.6	2.3
Perp.	699.9	695.9	728.5	746.9	15.3	2.1
All samples	661.9	690.9	723.8	755.3	17.8	2.5
G_v (MPa)						
18 mm thick.	520.8	506.2	587.6	665.7	42.1	7.2
Para.	527.6	500.4	585.5	639.2	40.0	6.8
Perp.	520.8	490.7	589.6	665.7	46.5	7.9
25 mm thick.	455.4	452.7	512.0	575.1	30.7	6.0
Para.	455.4	428.5	498.2	543.0	32.8	6.6
Perp.	494.1	478.2	525.7	575.1	22.4	4.3
All samples	455.4	452.5	549.8	665.7	52.8	9.6
f_v (MPa)						
18 mm thick.	10.5	10.5	12.0	13.1	0.7	6.1
Para.	10.5	10.1	11.8	12.9	0.8	6.7
Perp.	11.0	10.7	12.1	13.1	0.7	5.6
25 mm thick.	10.0	10.1	11.6	12.8	0.8	7.0
Para.	10.0	9.6	11.5	12.4	0.9	7.7
Perp.	10.8	10.2	11.8	12.8	0.7	6.2
All samples	10.0	10.4	11.8	13.1	0.8	6.6

displacement curves are presented in the upper part. The displacement represents the relative displacement of the two points as it was described before in the Section "Mechanical Properties Calculation" for each side of the panel (front and rear) analogously to the method described in EN 789. The two selected points are also visible on the displacements fields. The different steps for which displacements field are plotted correspond respectively to results under a load equal to $0.1F_{max}$, $0.4F_{max}$, $0.8F_{max}$ and after failure under a residual load equal to $0.63F_{max}$. For each step displacement fields in x-direction for both sides (Ux Front and Ux Rear) and in y-direction (Uy Front and Uy Rear) are presented. The measured displacement on both sides were really close to each other. This result can be seen on the load-displacement curve as well as on the displacement fields.

One of the advantages of DIC is that it allows to check the validity of the solicitation. The comparison of the displacements fields obtained on the front side by DIC and by FEM is presented in Fig. 8. The comparison is made at the same load and corresponds to the third step described previously (i.e at $0.8F_{max}$). The comparison is done on the displacements fields where the rigid body motion had been removed. It can be seen that the displacements fields in both directions were similar quantitatively.

The lower part of Fig. 7 shows that this method is an effective way to identify the failure position. The failure position computed on the two sides of every samples is presented in Fig. 9. The distance from the centre and the actual failure path is comprised between -39.1 and 32.1 mm. Therefore, every sample has been accepted for the computation of the shear strength since no failure occurred in another way than in shear between the two rails. The average absolute distance between the failure and the geometric centre is equal to 12.4 mm which can be considered low enough to use the shear length l in the calculation of the shear strength.

Mechanical Properties Analysis

Figure 10 presents the results of the shear modulus for the 36 panels, the upper part for the 18 mm thick panels and the lower part for the 25 mm thick panels. The blue dashed line represents the shear modulus calculated on the

Fig. 11 Comparison between experimental values and equivalencies given in EN 12369-2
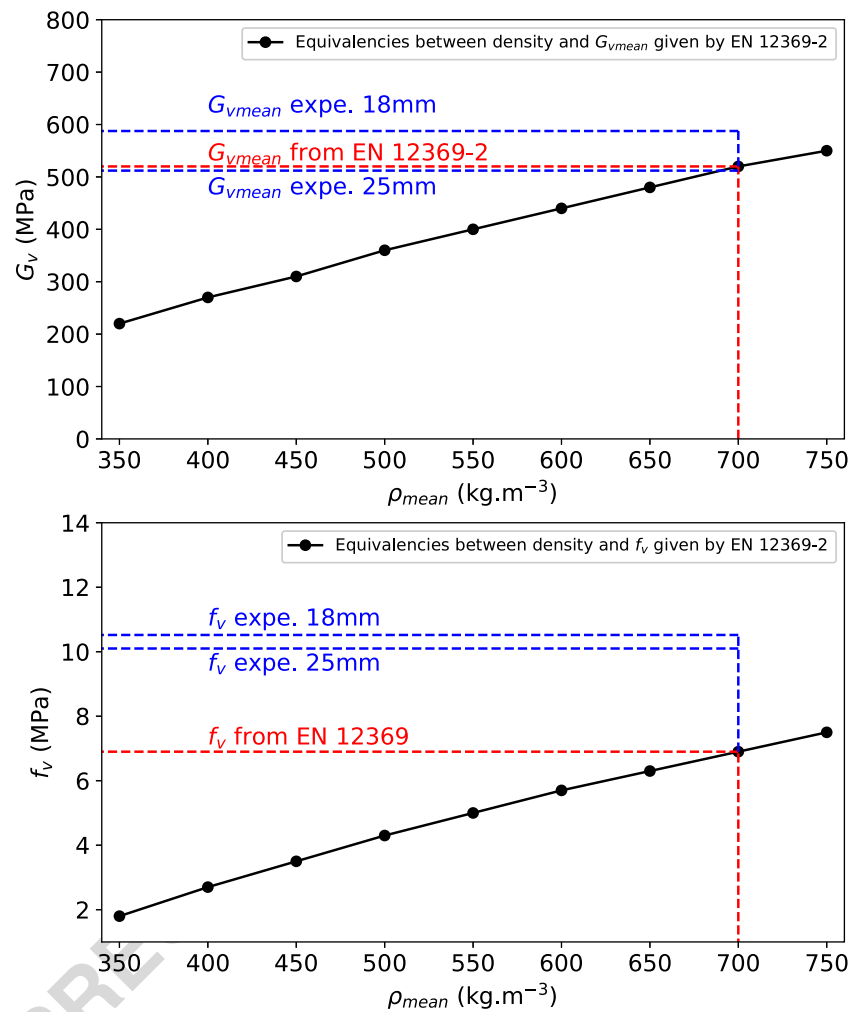
basis of the DIC measurement on the front side, the red dashed line the one measured on the rear side, and the black plain line their mean value. Those results show that the difference between the shear modulus calculated on both sides is low. Indeed, the mean relative variation is equal to only 3.6% with a maximal relative variation equal to 13.7%. These percentages represent a mean absolute variation of 20.2 MPa and a maximal variation of 76.5 MPa on the shear modulus.

Descriptive statistics for the density, the shear modulus, and the shear strength are given in Table 2. The mean value for 18 mm thick and 25 mm thick panel were respectively equal to 717.7 and 729.8 kg.m^{-3}. The corresponding coefficients of variation were equal to 2.5 and 2.1% which is consistent with the literature in the case of beech [22–25]. The mean shear modulus G_v is respectively equal to 587.6 and 512.0 MPa for 18 and 25 mm thick samples. This result is consistent with the results based on the numerical model. In addition, the samples from the type Perp. have a higher shear modulus in every case which is also in accordance with the numerical model. Finally, the average

shear strength f_v and its corresponding variability were really close for every thicknesses and sample types; the global averaged shear strength is approximately equal to 12 MPa.

Interest of the Test Realization Over Density Based Equivalencies

The survey conducted on the plywood panel manufacturers' performances reports in Europe revealed that the majority of producers use density-based equivalencies given by the standards [8] to provide shear properties. The average densities for 18 mm and 25 mm thick panels were respectively 717 and 729 kg.m^{-3}, according to the same standard the value of 700 kg.m^{-3} must be used (N.B: its lower limit must be used). Using this threshold, the shear properties could be taken equal to 520 and 6.9 MPa for the shear modulus and the shear strength respectively. Figure 11 presents the comparison between values obtained experimentally in this study and the values taken from the equivalencies applying the standards. These results show

that the realization of the shear tests is favorable or at least equivalent in the case of the shear modulus and always favorable for the calculation of the shear strength.

Conclusion

This study proposed a modified of the two rails shear test in a more functional configuration, meaning without the use of a bulky apparatus. The validity of the tests has been shown by the use of full field measurement using DIC. Nevertheless, the test could still be performed using a simpler measurement device such as a LVDT in the tilted proposed configuration. The interest of the realization of these tests has been highlighted in comparison with the use of equivalences based on the measurement of the average density. In any case, the measurements taken from the tests can lead to the declaration of shear properties equivalent or even greater than those expected by the standard and thus enhance significantly the valorization of beech plywood.

Compliance with Ethical Standards

Conflict of interests The authors declare that they have no conflict of interest.

References

1. Dobbin McNatt J (1969) Rail shear test for evaluating edgewise shear properties of wood base panel products. tech. rep., U.S.D.A Forest Service, Forest Products Laboratory. Madison
2. Munthe B, Ethington RL (1968) Method for evaluating shear properties of wood. US Department of Agriculture, Forest Service, Forest Products Laboratory
3. Rune Z (1994) Evaluation Of test methods for wood based panels. Determination of shear modulus and shear strangth. Tech. Rep. Nordtest Project No. 1060–92, Swedish National Testing and Research Institute
4. Ehlbeck J, Colling F (1984) Determination of panel shear strength and shear modulus of beech plywood in structural sizes. (SWITZERLAND)
5. Wilson CR, Parasin AV (1979) A comparison of plywood modulus of rigidity determined by the ASTM and RILEM/CIB-3tt test methods, (Austria)
6. Booth LG, Kuipers J, Noren B, Wilson CR (1977) Methods of test for the determination of mechanical properties of plywood, (Sweden)
7. CEN (2005) EN 789 timber structures - test methods - determination of mechanical properties of wood based panels
8. CEN (2011) EN 12369-2 wood-based panels - characteristic values for structural design - Part 2: Plywood
9. Yoshihara H, Yoshinobu M (2015) Young's modulus and shear modulus of solid wood measured by the flexural vibration test of specimens with large height/length ratios. Holzforschung 69(4):493–499
10. Cavalli A, Marcon B, Cibecchini D, Mazzanti P, Fioravanti M, Procino L, Togni M (2017) Dynamic excitation and FE analysis to assess the shear modulus of structural timber. Mater Struct 50(2):130
11. Vacher P, Dumoulin S, Morestin F, Mguil-Touchal S (1999) Bidimensional strain measurement using digital images. Proc Inst Mech Eng C J Mech Eng Sci 213(8):811–817
12. Wattrisse B, Chrysochoos A, Muracciole J-M, Némoz-Gaillard M (2001) Analysis of strain localization during tensile tests by digital image correlation. Exp Mech 41(1):29–39
13. Sutton M, Wolters W, Peters W, Ranson W, McNeill S (1983) Determination of displacements using an improved digital correlation method. Image Vis Comput 1(3):133–139
14. Bruck H, McNeill S, Sutton MA, Peters W (1989) Digital image correlation using newton-Raphson method of partial differential correction. Exp Mech 29(3):261–267
15. Bornert M, Brémand F, Doumalin P, Dupré J-C, Fazzini M, Grédiac M, Hild F, Mistou S, Molimard J, Orteu J-J, Robert L, Surrel Y, Vacher P, Wattrisse B (2009) Assessment of digital image correlation measurement errors: methodology and results. Exp Mech 49(3):353–370
16. Jeong GY, Zink-Sharp A, Hindman DP (2009) Tensile properties of earlywood and latewood from loblolly pine (Pinus taeda) using digital image correlation. Wood Fiber Sci 41(1):51–63
17. Zink AG, Davidson RW, Hanna RB (2007) Strain measurement in wood using a digital image correlation technique. Wood Fiber Sci 27(4):346–359
18. Haldar S, Gheewala N, Grande-Allen K, Sutton M, Bruck H (2011) Multi-scale mechanical characterization of palmetto wood using digital image correlation to develop a template for biologically-inspired polymer composites. Exp Mech 51(4):575–589
19. CEA (2019) Cast3m
20. Guitard D (1987) Mécanique du matériau bois et composites. NABLA, cepadues ed.
21. Bergman R, Cai Z, Carll CG, Clausen CA, Dietenberger MA, Falk RH, Frihart CR, Glass SV, Hunt CG, Ibach RE (2010) Wood handbook: Wood as an engineering material. Forest Products Laboratory
22. Gérard J, Guibal D, Paradis S, Vernay M, Beauchêne J, Brancheriau L, Châlon I, Daigremont C, Détienne P, Fouquet D, Langbour P, Lotte S, Thévenon M-F, Méjean C, Thibaut A (2011) Tropix 7
23. Pöhler E, Klingner R, Künniger T (2006) Beech (Fagus sylvatica L.) – Technological properties, adhesion behaviour and colour stability with and without coatings of the red heartwood. Annals Forest Sci 63(2):129–137
24. Viguier J, Bourgeay C, Rohumaa A, Pot G, Denaud L (2018) An innovative method based on grain angle measurement to sort veneer and predict mechanical properties of beech laminated veneer lumber. Constr Build Mater 181:146–155
25. Viguier J, Marcon B, Girardon S, Denaud L (2017) Effect of forestry management and veneer defects identified by x-ray analysis on mechanical properties of laminated veneer lumber beams made of beech. BioResources